

Three-dimensional modelling of artificial caves for geomechanical analysis

Alessandra Spadaro¹, Marco Piras¹, Nives Grasso¹, Piernicola Lollino², Alessandro Parisi³, Daniele Giordan⁴

¹ Dept. of Environment, Land and Infrastructure Engineering (DIATI), Politecnico di Torino, Turin, Italy –
(alessandra.spadaro, marco.piras, nives.grasso)@polito.it

² Department of Earth and Geoenvironmental Sciences, University of Bari, Bari, Italy – piernicola.lollino@uniba.it

³ Association "Gravina Sotterranea" – Geophysical Applications Processing - GAP s.r.l., Bari, Italy – alessandro.paris@gapsrl.eu

⁴ Research Institute for Geo-hydrological Protection (IRPI), Italian National Research Council, Turin, Italy – daniele.giordan@cnr.it

Keywords: Underground survey, 3D data analysis, LiDAR technology, Spherical photogrammetry, 360° camera, Geo-mechanics.

Abstract

Accurate cave surveying is crucial for understanding their genesis, current state, and potential hazards, especially in challenging environments marked by limited accessibility and poor visibility. This study applies geomatics techniques, including Terrestrial Laser Scanning (TLS), SLAM-based Mobile Mapping Systems (MMS), and digital photogrammetry, to create three-dimensional models of artificial caves in Gravina in Puglia, Apulia region, southern Italy. The research aims to assess these methodologies' accuracy, reliability, and performance for structural monitoring and hazard assessment. Despite challenges such as rough conditions, limited accessibility and poor visibility, the study reveals promising insights into the capabilities of these techniques for efficient surveying in complex underground environments. While highlighting the potential of MMS for cost-effective and rapid data acquisition, digital photogrammetry using spherical cameras also emerges as a viable alternative, offering comprehensive data collection capabilities with minimal capture time. Further research is warranted to optimize these techniques for enhanced hazard assessment and structural monitoring in challenging underground environments.

1. Introduction

Accurate cave surveying is frequently challenging due to the rough conditions and limited accessibility of the study area as well as the challenges posed by factors such as complex geology and poor visibility. Nevertheless, accurate surveys have always been critical to investigating their genesis and the changes that led to their current state and to providing tools and helpful information for hazard assessment (Idrees and Pradhan, 2016). Geomatics' contribution has become extremely substantial, with the widespread implementation of tools and methodologies for different purposes, such as data acquisition, analysis, and geospatial data management. The creation of three-dimensional models allows to understand the spatial distribution of complex and difficult-to-access environments, as well as for geomorphological observation (Dewaele et al., 2018), identification of areas at high risk of structural degradation (Domej et al., 2022) and geomechanical stability assessment (Fazio et al. 2017). Terrestrial laser scanners (TLS) have been widely used to map underground environments and even caves (Idrees and Pradhan, 2016; Castellanza et al. 2018; Giordan et al., 2021; Cardia et al., 2021). In other cases, some other instruments can be used, starting from Simultaneous Localization And Mapping (SLAM) based portable instruments (Pisoni, I., 2022; Tanduo B., 2023) and digital photogrammetry using 360-degree cameras (Janiszewski et al., 2022). During this research, the following aspects will be examined.

Firstly, the creation of metrically accurate three-dimensional models with medium and high precision will be pursued. This aims to (i) enhance the understanding of the planimetric development of the artificial underground cavities in Gravina di Puglia, Apulia, Italy, a site of significant architectural, historical, and cultural importance, and (ii) facilitate studies integrating geological and geomechanical data for structural monitoring, subsidence analysis, and assessment of areas prone to collapse. Secondly, the performance of SLAM and VIS geomatic techniques for three-dimensional model reconstruction and geomechanical analysis will be compared and discussed in

terms of accuracy, acquisition and processing time, portability, and autonomy.

1.1 Artificial caves in Gravina in Puglia, Apulia region, southern Italy

The "Gravine" are spectacular geological formations characterized by deep valley incisions with steep and sub-vertical walls, and they represent a true natural treasure and a cultural heritage of inestimable value, which is typical in the Apulia region. Their development is a complex and articulated combination of settlement and cultural processes from different epochs and connotations, tightly integrated into the current urban fabric. The Calcarenite di Gravina, a limestone formation renowned for its excellent mechanical properties, has served as a foundational element in the construction and evolution of settlements along the Gravine. Over time, various types of residential structures have been developed within the historic center of Gravina in Puglia (Figure 1), intricately linked to the soft limestone substrate. These include dwellings directly carved into the limestone, such as cave houses and basements, as well as structures where vertical excavation was employed to extract limestone blocks for construction above ground (Figure 2). This architectural evolution has given rise to a multitude of subterranean spaces beneath individual dwellings, fulfilling diverse functions ranging from wine cellars to rainwater cisterns. Furthermore, the subterranean spaces beneath the main squares and streets of Gravina's ancient inhabited center offer valuable insights into the dynamic interaction between human settlement and geological features. Historical instabilities, driven by factors such as conflicts, invasions, and disease outbreaks have led to demographic shifts and urbanization processes, significantly modifying the urban landscape. These include the creation of silos for granary storage and the excavation of public cisterns for water collection, reflecting the adaptive response of human societies to environmental challenges within this geological context. Despite their cultural and historical significance, a portion of this heritage still needs



Figure 1. The historic center of Gravina in Puglia, Apulia region, Southern Italy.

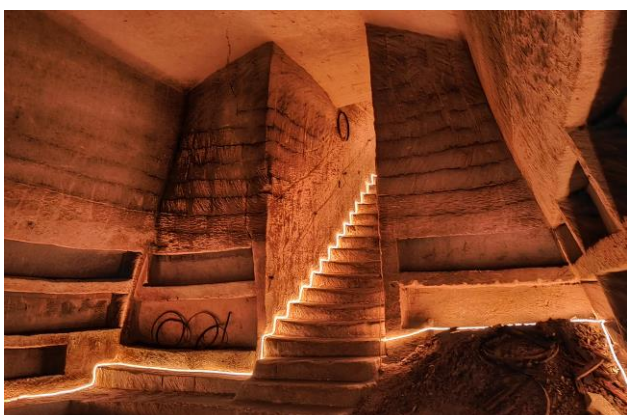


Figure 2. Image within the 'Cantina del Principe' artificial cave, research case study, revealing remnants of block excavation on the walls.

to be explored, and what has been surveyed is sometimes in a precarious state of conservation, creating a risk condition for the resident populations and the overlying structures and infrastructures. Hence, the need arises to systematically map and document these cavities to comprehensively assess their structural integrity, potential hazards, and interaction with the overlying urbanized environment, as well as to conduct structural and geomechanical analyses. Geomatic techniques provide valuable support in creating three-dimensional models, aiding in the understanding and management of these complex environments.

2. Material and methods

The survey campaign was carried out in May 2023 in the historic center of Gravina in Puglia, Apulia region. The object of survey and analysis is an anthropic cavity named the "Cantina del Principe" (Figure 2), located within the courtyard of some buildings (latitude 40° 49'01.3"N, longitude 16°25'03.5"E, elevation 355 masl). It is accessible via adjacent chambers, a corridor, and a flight of stairs. The "Cantina" is characterized by a single chamber with dimensions of approximately 7 meters in height, 13 meters in length, and 6 meters in thickness.

Three different techniques of three-dimensional surveying have been employed.

Terrestrial Laser Scanner (TLS) using the Leica RTC360, a LiDAR based on VIS (Visual Inertial System) solution for real-time cloud data registration.

SLAM-based Mobile Mapping System (MMS) using KAARTA Stencil 2, composed of a Velodyne VLP-16, a MEMS (Micro Electronic Mechanical System) inertial platform, and a feature tracker camera connected to a processor Intel Core i7.

Tables 1 and 2 have some specifications regarding the LiDAR instrument used, respectively, Leica RTC360 and KAARTA Stencil 2.

Table 1. Leica RTC360 main specifications.




 *for the considered dataset	Acquisition speed	Up to 2,000,000 pts/s
	Field of view	360° (horiz.) / 300° (vert.)
	Range	Min. 0.5 - up to 130 m
	Resolution*	Medium: 6 mm at 10 m
	LiDAR Accuracy	Angular: 18" Range: 1.0 mm + 10 ppm
	3D point accuracy	1.9 mm @ 10 m
	Weight	5.2 kg (without batteries)

Table 2. KAARTA Stencil 2 main specifications.

	Acquisition speed	Up to 300,000 pts/s
	Field of view	30° (horiz.) / 360° (vert.)
	Range	Min. 1 - up to 100 m
	Resolution	Medium: 6 mm at 10 m
	LiDAR Accuracy	± 30 mm
	Weight	1,7 kg

Even digital photogrammetry has been considered, using the spherical camera Insta360 One RS 1-inch edition co-engineered with Leica. Table 3 shows some camera specifications. The 360° module covers the entire 360x180° scene and consists of two fisheye sensors. The camera is equipped with a gyroscope to stabilize images in all conditions.

Table 3. Insta360 One RS 1-inch edition main specifications.

	Image resolution	21 MPx
	Focal length (equ.)	6.52 mm
	Focal Aperture	F2.2
	Video Resolution	3840x1920@30/25/24fps 3040x1520@50fps
	ISO Range Video	100-3200
	Weight	0, 239 kg

The analyses were conducted using a computational system equipped with an Intel(R) Core(TM) i7-6850K CPU @ 3.60GHz, 128 GB of RAM, an NVIDIA Quadro M2000 GPU, and running on the Windows 1, 64-bit platform.

2.1 TLS data acquisition and processing

The TLS data served as ground truth for assessing the accuracy and quality of the SLAM-MMS and spherical photogrammetry (SP) point clouds. A total of fifteen static scans were conducted, spanning from the courtyard to the main chamber of the "Cantina del Principe", as shown in Figure 3. The acquisition quality was set to "Medium," with a point spacing of 6 mm at 10 m and an acquisition time of 1 minute and 51 seconds per scan, including capturing spherical HDR images for point cloud coloring. Leveraging the VIS solution, the TLS Leica RTC360 facilitated real-time point cloud registration, thereby reducing post-processing time through automatic point cloud alignment based on continuous monitoring of scanner movement between setups. Furthermore, using Leica's Cyclone FIELD 360 software enabled direct 3D data management in the field, streamlining the entire acquisition process and minimizing the likelihood of errors during the acquisition phase. Subsequently, TLS data underwent post-processing using Leica's Cyclone REGISTER 360 software, optimizing it with the Iterative Closest Point (ICP) algorithm. This yielded an ICP registration error of 0.003 m, resulting in a final point cloud (Figure 3) comprising approximately 30,000,000 points with a file size of 800 MB and achieving a local accuracy of 3 mm. The acquisition phase spanned approximately 45 minutes, while the processing phase required around 2 hours.

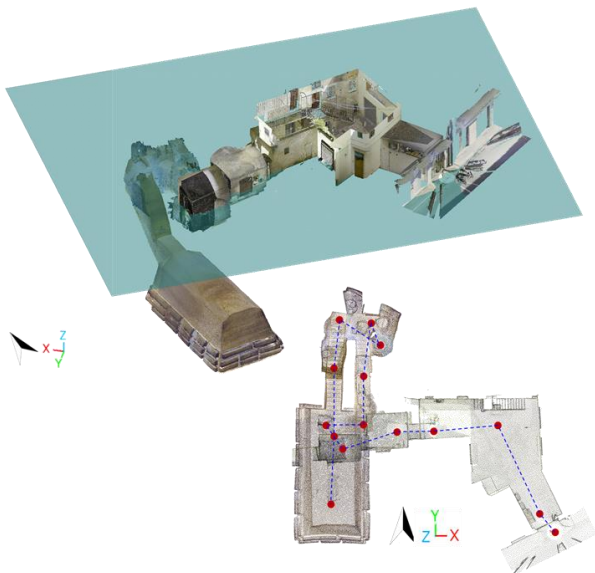


Figure 3. The TLS point cloud, which is used as a reference cloud, is shown. In planimetry, the red circles represent the different scan positions.

2.2 MMS data acquisition and processing

The SLAM method was employed with the MMS KAARTA Stencil 2, a 3D rapid mapping standalone system (Table 2), characterized by its relatively low cost compared to TLS systems and compact size, capable of real-time position. Its measurement principle combines laser range data, feature tracker data, and image information to estimate 6-DOF motion and record LiDAR-acquired points. The data processing follows a two-step workflow: first, visual-inertial odometry algorithms integrate vision and IMU for motion estimation optimization, associating depth information of features and registering laser points in a local system using speed information from odometry. A mapping algorithm then detects geometric features in the point cloud and matches them to optimize registration using pose constraints. This allows using the instrument solely with lidar-odometry, eliminating the need for image-based feature tracking but with an increased risk of positioning errors. In this case study, the Stencil 2 was mounted on a small pole and connected to a screen for real-time data acquisition verification (Figure 4). The scan started and ended at the same point to execute the Loop Closure algorithm; the scan acquisition lasted 4 minutes and 24 seconds. Post-processing utilized proprietary algorithms to simulate acquisition at a lower speed, enhancing trajectory estimation and point cloud registration accuracy, with a processing time of 7 minutes. The final MMS point cloud (Figure 5), comprising approximately 64,000,000 points (file size 1.5 GB), has an estimated trajectory of 159 m.

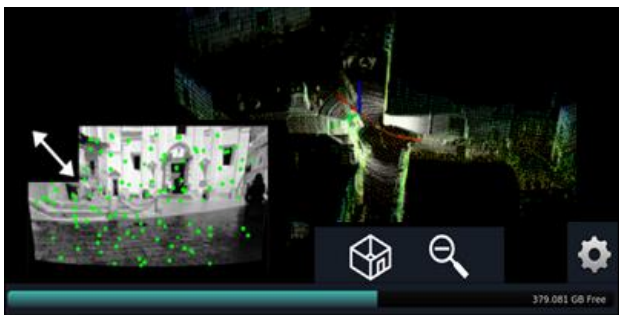


Figure 4. Real-time 3D point cloud using SLAM-MMS.

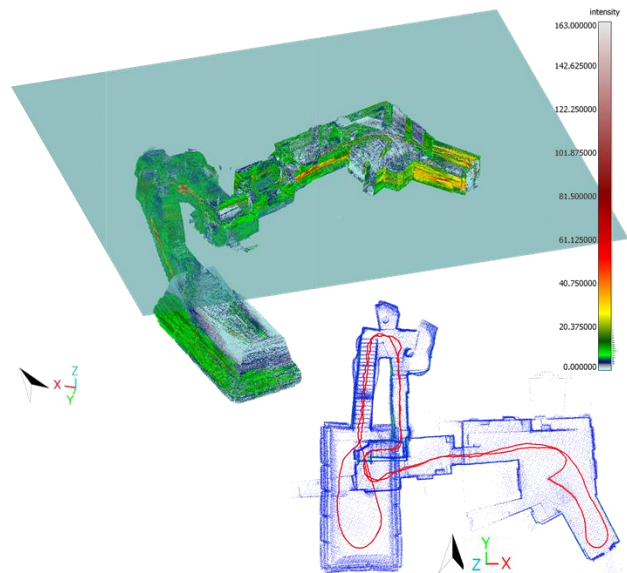


Figure 5. The SLAM-MMS point cloud is displayed. In planimetry, the computed trajectory is represented in red.

2.3 Digital photogrammetry with 360-degree camera

A 360-degree camera typically simplifies data acquisition compared to traditional close-range photogrammetry approaches based on frame cameras. However, it's crucial to carefully plan each sensor's acquisition strategy. There are three main strategies for capturing 360-degree images for Structure from Motion (SfM) processing: still images, time-lapse, and video (Teppati Losè et al., 2021). For the "Cantina del Principe" survey, the third strategy based on video acquisition was chosen due to its speed and cost-effectiveness. Videos were recorded at the maximum resolution of 6K (30 fps) using the Insta360 One RS 1-inch edition co-engineered with Leica. The camera was mounted on a pole support approximately 15 cm high and situated approximately 30–40 cm above the operator's head, effectively minimizing the operator's visibility within the camera's field of view (Figure 6). Due to the inadequate lighting conditions in the survey area, the operator was outfitted with LED light strips and a front-facing camera. The video was recorded with a one-way walk from the courtyard to the main chamber, lasting around 3 and a half minutes. Regarding data storage, Insta360 spherical cameras save dual-fisheye videos in ".insv" proprietary format, with each sensor saved in a separate file. In addition to video data, these files contain metadata, including gyroscope data. A crucial step in spherical photogrammetric processing is the stitching phase, which combines multiple single images or video frames into a mosaic virtual image or video. In Figure 6, a stitched frame extracted from a video acquired in "Cantina del Principe".

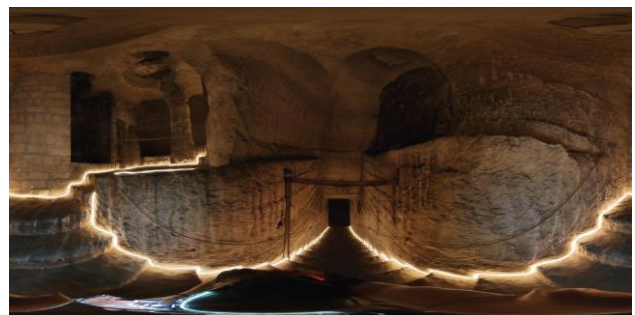


Figure 6. Stitched frame extracted from a 360° video.

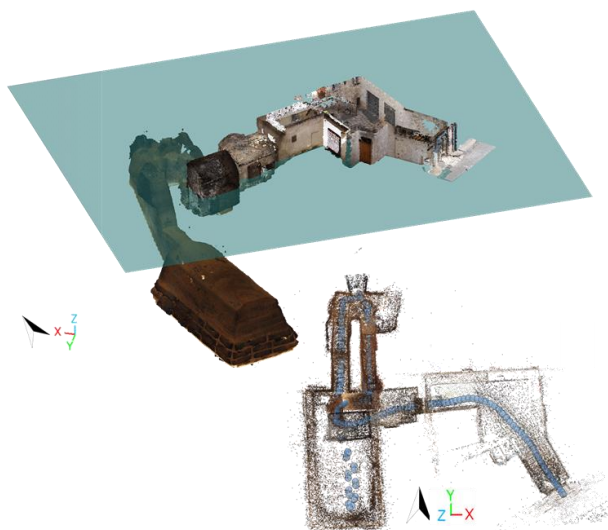


Figure 7. The point cloud obtained with spherical photogrammetry (SP) is shown. In planimetry, the blue spheres represent the position of the extracted frames used for the construction of the photogrammetric block.

This phase can be automatically performed using various commercial and open-source software solutions. However, in recent years, commercially available 360-degree cameras come with their own dedicated stitching software. For the Insta360 One RS 1-inch edition, Insta360 Studio software was used to perform stitching, color correction and stabilization. The result is a stitched video in 2:1 equirectangular projection in “.mp4” format, from which frames can be extracted to be used for photogrammetric processing phases (Figure 6).

The frame extraction and photogrammetric processing, following the standard SfM pipeline, were performed using the commercial solution Agisoft Metashape. Specifically, one frame was extracted every 30, totaling 226 images, with a processing time of 10 minutes. The main parameters used for photogrammetric processing are detailed in Table 4. The metric accuracy of the processing was assessed using 9 control points, with 6 used as Ground Control Points and 3 as Check Points.

Table 4. Some information on the SfM processing using the 360° camera.

Aligned images	GSD (mm/pix)	RMSE GCPs (m)	RMSE CPs (m)
226/226	1,32	0.033 m	0.068 m

Alignment and creation of the sparse point cloud, set to medium quality, with 194,248 Tie Points, took 13 minutes, while creation of the dense point cloud (77.0 M pts, 1.90 GB), showed in Figure 7, took 1 hour and 20 minutes.

3. Results and data analysis

The three-dimensional models were elaborated and compared qualitatively and quantitatively based on various criteria, including accuracy and reliability of results, the point cloud's completeness, and the geometrical reconstruction's quality. Additionally, assessments have been conducted regarding equipment cost, acquisition and processing time, portability, and autonomy.

The dense point clouds obtained with the MMS SLAM KAARTA Stencil 2 and the Insta360 One RS 1-inch edition were utilized to assess mapping capabilities in complex indoor underground environments, with TLS data serving as a reference. Regarding metric accuracy, assessments were made using the C2C (Cloud-to-Cloud) distance analysis and

comparison along transverse and longitudinal sections within the anthropic cavity.

3.1 C2C analysis

The Cloud-to-Cloud (C2C) analysis was conducted using the open-source software CloudCompare. The C2C tool leverages the Nearest Neighbor algorithm to calculate the Euclidean distance between each point of the compared cloud and the nearest point of the reference cloud.

The TLS point cloud used as ground truth was downsampled to one point per centimeter, starting from a medium resolution of one point every 6 mm at 10 meters. This was done to streamline data management, considering that the accuracy and conventional tolerance for the nominal representational scale of 1:100 are 2 and 4 cm, respectively.

At this point, it was necessary to register the models generated by MMS and SP in a reference system consistent with the TLS reference model. In this regard, CloudCompare offers several tools: a rough registration can be performed through pairs of equivalent points identified in the point cloud to be registered and in the reference one; subsequently, the automatic method based on the Iterative Closest Point (ICP) algorithm (Besl and McKay, 1992) allows the two clouds to be very finely recorded. This procedure was performed for both models.

The C2C tool was launched by setting the points distant from the reference model more than 50 cm as outliers, since the errors that interest us are lower than this limit. The final RMSE was 3.18 cm for the MMS point cloud and 11.3 cm for the SP point cloud.

Figure 8 shows the C2C distances of MMS and SP cloud with TLS reference one and the C2C distribution histograms. The computation of the differences confirmed the metrical accuracy of the model estimated by the SLAM MMS Stencil 2; indeed, in correspondence with the ceiling, the point cloud is quite sparse and noisy due to the limited field of view of the instrument. Regarding the SP point cloud, the most significant computational difference is noticed in the southern wall of the anthropic cavity. This is due to several factors: a limited number of spherical images used for photogrammetric reconstruction because of the acquisition trajectory confined to the central part of the cavity (Figure 7). Additionally, the traversal speed of the specific section was higher compared to the rest of the cavity, attributable to its more uniform environment, resulting in the extraction of fewer frames. Improved planning and execution during the spherical video acquisition phase could have helped mitigate this issue.

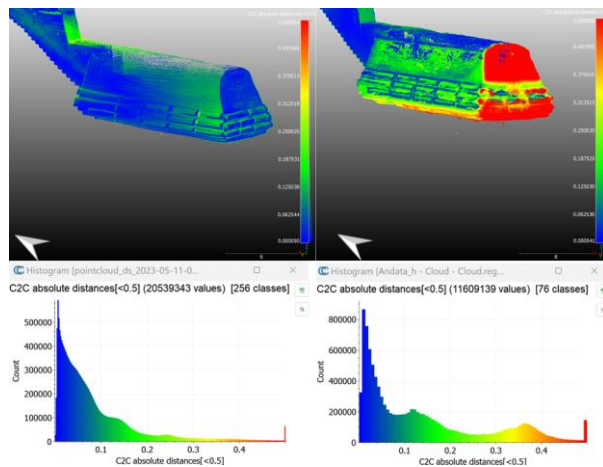


Figure 8. On the left, point cloud comparison between the MMS and the reference model. On the right, point cloud comparison between the SP and the reference model.

3.2 Cross-section analysis

A second analysis compared profiles extracted by MMS, SP, and TLS reference point clouds. The evaluation was conducted in order to verify the deviation from the reference point cloud in the correspondence of the main chamber. Using the specific tool in CloudCompare, one longitudinal and one transversal 5 cm-wide slice were extracted from each model. Figure 9 shows slices extracted from the reference point cloud. Figure 10 depicts longitudinal and transversal sections for comparing the three models, featuring an enlarged view of the area outlined with dashed lines.

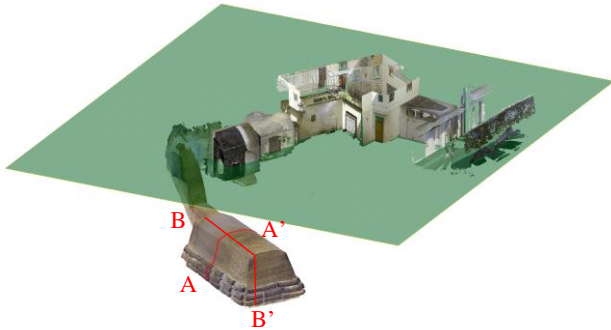


Figure 9. The TLS reference point cloud is displayed, with the highlighted section (in red) indicating the section under analysis.

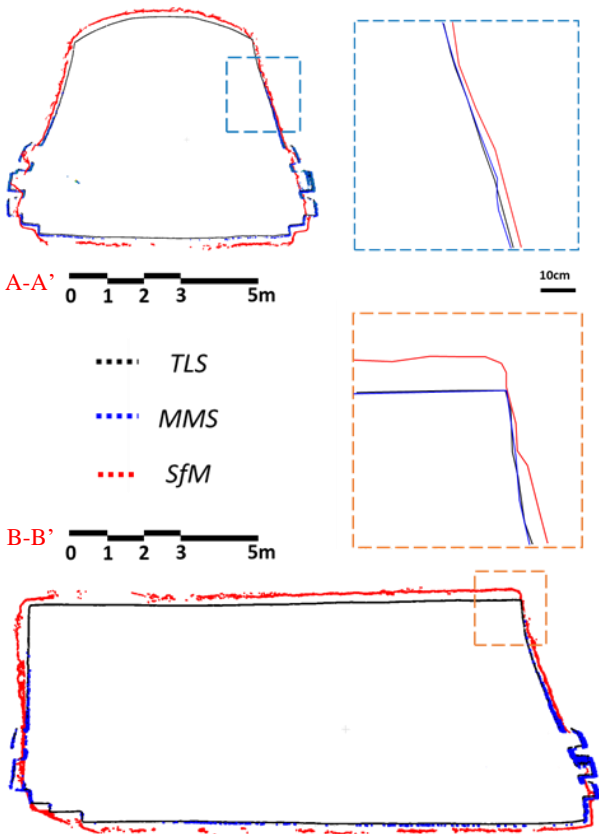


Figure 10. A comparison between the TLS reference point cloud (in black), MMS point clouds (in blue), and spherical photogrammetry (in red) is shown. The right boxes shows an enlarged view of the areas outlined in dashed blue and orange.

3.3 MMS point cloud colouring

The point cloud obtained with the SLAM Stencil 2 instrument doesn't contain radiometric data as the integrated camera in the acquisition system captures only black-and-white images. We opted for the model generated through processing spherical images to introduce radiometric information to the MMS point cloud. Using a dedicated tool in CloudCompare it is possible to interpolate the color of another entity in order to add the radiometric information to the points of a chosen entity. This computation was completed in about 2 minutes. Figure 11 initially displays the MMS point cloud with the intensity scalar field, followed by the same MMS point cloud colored using the radiometric information obtained from the spherical images.



Figure 11. In the upper part, the MMS point cloud shows the intensity scalar field, the LiDAR intensity function recorded as the laser beam's return strength. At the bottom, the same point cloud is colored using the radiometric information extracted from the SP model.

4. Conclusion and future work

This study aimed to evaluate and compare three different techniques for three-dimensional modeling for geomechanical analysis of anthropic cavities in the historic center of Gravina in Puglia, southern Italy. Specifically, Terrestrial Laser Scanning (TLS), SLAM-based Mobile Mapping System (MMS), and digital photogrammetry using a 360-degree camera were employed.

The accuracy and reliability of the three-dimensional models obtained through TLS, MMS, and spherical photogrammetry were assessed through Cloud-to-Cloud (C2C) analysis and cross-section analysis. The TLS reference point cloud provided a benchmark for comparison, with the models obtained using MMS based on SLAM and spherical photogrammetry.

The MMS demonstrated commendable accuracy in such a complex site for a nominal scale not larger than 1:100. However, limitations were observed in the areas with a restricted field of view of the instrument, resulting in sparser and noisier point clouds. Similarly, digital photogrammetry emerged as a viable alternative, offering comprehensive data collection capabilities with minimal capture time, despite some inconsistencies in model reconstruction, especially in areas with inadequate image coverage or higher traversal speeds during video acquisition. The equipment cost varies significantly among the three techniques. TLS systems are relatively expensive due to their advanced technology and high precision capabilities. On the other hand, SLAM-based MMS solutions like the KAARTA Stencil 2 offer a more cost-effective alternative, albeit with slightly lower accuracy. Digital photogrammetry using a 360-degree camera is the most budget-friendly option, although it requires known coordinate points to achieve a metrically accurate model. Regarding the acquisition and processing time, TLS data acquisition is relatively time-consuming, particularly for larger survey areas, although advancements such as real-time cloud data registration can expedite the process. Processing TLS data also requires significant computational resources and time. In contrast, SLAM-based MMS offers rapid data acquisition, with real-time processing capabilities significantly reducing post-processing time. Digital photogrammetry with a 360-degree camera allows for quick data acquisition, but processing time may vary depending on the computational device employed for analysis. Also, portability and autonomy are crucial factors, especially for surveys in challenging environments. TLS systems are typically bulky and require a stable setup, limiting their portability and autonomy. In contrast, SLAM-based MMS solutions are more compact and mobile, allowing greater flexibility in surveying complex environments or confined spaces. Digital photogrammetry using a 360-degree camera offers the highest level of portability and autonomy, as the equipment is lightweight and easily transportable, making it suitable for field surveys in diverse locations. Overall, good performance was achieved regarding acquisition and processing time, data accuracy, ease of use, and portability for SLAM and VIS systems. However, as these are complex environments with restricted spaces and significant elevation changes, limited brightness conditions may affect the quality of data acquired through these solutions. In terms of future applications of the acquired data, there are several interesting possibilities. One avenue involves utilizing the three-dimensional models to conduct finite element geomechanical analyses (Figure 12) with different levels of resolution. This approach allows for a detailed examination of structural integrity and potential hazards within the underground cavities. Additionally, the models can be instrumental in evaluating the stability of the entire cavity-structure system, providing valuable insights into the interaction dynamics between underground heritage sites and the urbanized areas above ground.

Acknowledgements

This study was carried out within the RETURN Extended Partnership and received funding from the European Union Next GenerationEU (National Recovery and Resilience Plan NRRP, Mission 4, Component 2, Investment 1.3 D.D. 1243 2/8/2022, PE0000005) SPOKE 6 - TS2. Moreover, this study is part of the collaboration agreement "Spatial analysis of the underground caves of historical, artistic and cultural value in the historic center of Gravina in Puglia (BA) in relation to the built-up area" between the cultural association "Gravina Sotterranea" and the Research Institute for Geo-hydrological Protection (IRPI), Italian National Research Council.

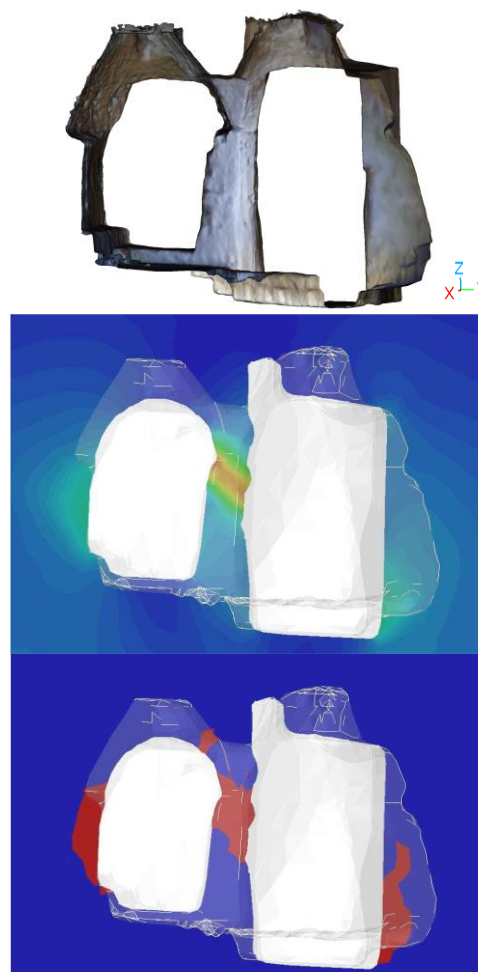


Figure 12. On the top, the high-resolution 3D model is used for geomechanical analysis on a pillar. In the center, finite element model results show the deviatoric deformations and, at the bottom, the yielding zones of the studied pillar.

References

- Idrees, M., Pradhan, B., 2016: A decade of modern cave surveying with terrestrial laser scanning: A review of sensors, method and application development. *International Journal of Speleology* 45(1): 71-88. doi.org/10.5038/1827-806X.45.1.1923
- DeWaele, J., Fabbri, S., Santagata, T., Chiarini, V., Columbu, A., Pisani, L., 2018: Geomorphological and speleogenetical observations using terrestrial laser scanning and 3D photogrammetry in a gypsum cave (Emilia Romagna, N. Italy). *Geomorphology*, 319,47–61. doi.org/10.1016/j.geomorph.2018.07.012.
- Domej, G., Previtali, M., Castellanza, R., Spizzichino, D., Crosta, G., Villa, A., Fusi, N., Elashvili, M., Margottini, C., 2022: High-Resolution 3D FEM Stability Analysis of the Sabareebi Cave Monastery, Georgia. *Rock Mechanics and Rock Engineering*. doi.org/55. 10.1007/s00603-022-02858-z.
- Fazio N.L., Perrotti M., Lollino P., Parise M., Vattano M., Madonia G., Di Maggio C., 2017: A three-dimensional back-analysis of the collapse of an underground cavity in soft rocks. *Engineering Geology*, 228, 301 – 311. doi.org/10.1016/j.enggeo.2017.08.014.

Castellanza R., Lollino P., Ciantia M., 2018: A methodological approach to assess the hazard of underground cavities subjected to environmental weathering. *Tunnelling and Underground Space Technology*, 82,278-292, doi: 10.1016/j.tust.2018.08.041.

Giordan, D., Godone, D., Baldo, M., Piras, M., Grasso, N., Zerbetto, R., 2021: Survey Solutions for 3D Acquisition and Representation of Artificial and Natural Caves. *Applied Sciences*, 11, 648. doi.org/10.3390/app11146482.

Cardia, S., Langella, F., Pagano, M., Palma, B., Sabato, L., Tropeano, M., Parise, M., 2023: 3D digital analysis for geo-structural monitoring and virtual documentation of the saint Michael cave in Minervino Murge, Bari (Italy). *Digital Applications in Archaeology and Cultural Heritage*. 32. doi.org/10.1016/j.daach.2023.e00308.

Pisoni, I.N., Cina, A., Grasso, N., Maschio, P., 2022: Techniques and Survey for 3D Modeling of Touristic Caves: Valdemino Case. *Geomatics for Green and Digital Transition. ASITA 2022*. doi.org/10.1007/978-3-031-17439-1_23

Tanduo, B., Chiabrande, F., Coluccia, L., Auriemma, R., 2023: Underground Heritage Documentation: the case study of Grotta Zinzulusa in Castro (Lecce-Italy). *The Int. Archives of the Photogram., Remote Sensing and Spatial Inform. Sciences*. 1527-1534. doi.org/10.5194/isprs-archives-XLVIII-M-2-2023-1527-2023.

Janiszewski, M., Torkan, M., Uotinen, L., Rinne, M., 2022: Rapid Photogrammetry with a 360-Degree Camera for Tunnel Mapping. *Remote Sens*. 14, 5494. doi.org/10.3390/rs14215494.

Kaarta, Kaarta, Instructions for Stencil®, 2018

Teppati Losè, L., Spanò, A., Anguissola, A, 2021: Geomatics Advanced Testings Flanking Archaeological Research: A Noteworthy Area in the Northern Necropolis of Hierapolis of Frigia (TK). *Editorial Universitat Politècnica de València*. doi.org/10.4995/arqueologica9.2021.12149

Besl, P., McKay, H.D., 1992. A method for registration of 3-D shapes. *IEEE Trans Pattern Anal Mach Intell. Pattern Analysis and Machine Intelligence*, IEEE Transactions on. 14. 239-256. 10.1109/34.121791.